

DTIC FILE COPY

②

UNCLASSIFIED

SECURITY CLASSIFICATION OF THIS PAGE

REPORT DOCUMENTATION PAGE

1a. REPORT SECURITY CLASSIFICATION UNCLASSIFIED		1b. RESTRICTIVE MARKINGS									
2a. SECURITY CLASSIFICATION AUTHORITY		3. DISTRIBUTION/AVAILABILITY OF REPORT Approved for public release; Distribution unlimited									
2b. DECLASSIFICATION/DOWNGRADING SCHEDULE											
4. PERFORMING ORGANIZATION REPORT NUMBER(S)		5. MONITORING ORGANIZATION REPORT NUMBER(S) <p style="text-align: center; font-weight: bold; font-size: 1.2em;">AFOSR-TR- 87-0296</p>									
6a. NAME OF PERFORMING ORGANIZATION University of Oregon	6b. OFFICE SYMBOL <i>(If applicable)</i>	7a. NAME OF MONITORING ORGANIZATION AFOSR/NP									
6c. ADDRESS (City, State and ZIP Code) Dept. of Physics & Chemical Physics Institute Eugene, OR 97403-1274		7b. ADDRESS (City, State and ZIP Code) Building 410 Bolling AFB DC 20332-6448									
8a. NAME OF FUNDING/SPONSORING ORGANIZATION AFOSR	8b. OFFICE SYMBOL <i>(If applicable)</i> NP	9. PROCUREMENT INSTRUMENT IDENTIFICATION NUMBER F49620-84-C-0039									
8c. ADDRESS (City, State and ZIP Code) Building 410 Bolling AFB DC 20332-6448		10. SOURCE OF FUNDING NOS. <table border="1" style="width: 100%; border-collapse: collapse; margin-top: 5px;"> <thead> <tr> <th style="width: 25%;">PROGRAM ELEMENT NO.</th> <th style="width: 25%;">PROJECT NO.</th> <th style="width: 25%;">TASK NO.</th> <th style="width: 25%;">WORK UNIT NO.</th> </tr> </thead> <tbody> <tr> <td style="text-align: center;">61102F</td> <td style="text-align: center;">2301</td> <td style="text-align: center;">A4</td> <td style="text-align: center;">N/A</td> </tr> </tbody> </table>		PROGRAM ELEMENT NO.	PROJECT NO.	TASK NO.	WORK UNIT NO.	61102F	2301	A4	N/A
PROGRAM ELEMENT NO.	PROJECT NO.	TASK NO.	WORK UNIT NO.								
61102F	2301	A4	N/A								
11. TITLE (Include Security Classification) RELATIVISTIC CALCULATIONS AND MEASUREMENTS OF ENERGIES, AUGER RATES AND LIFETIMES (U)											
12. PERSONAL AUTHOR(S) Dr Bernd Crasemann											
13a. TYPE OF REPORT FINAL	13b. TIME COVERED FROM 15 Jan 84 to 14 Jan 85	14. DATE OF REPORT (Yr., Mo., Day) 15 Feb 1985	15. PAGE COUNT 19								
16. SUPPLEMENTARY NOTATION											
17. COSATI CODES <table border="1" style="width: 100%; border-collapse: collapse; margin-top: 5px;"> <thead> <tr> <th style="width: 33%;">FIELD</th> <th style="width: 33%;">GROUP</th> <th style="width: 33%;">SUB. GR.</th> </tr> </thead> <tbody> <tr> <td> </td> <td> </td> <td> </td> </tr> </tbody> </table>		FIELD	GROUP	SUB. GR.				18. SUBJECT TERMS (Continue on reverse if necessary and identify by block number) quantum, relaticistic, electrodynamic			
FIELD	GROUP	SUB. GR.									
19. ABSTRACT (Continue on reverse if necessary and identify by block number) <p>Deep atomic hole states constitute a regime that has only recently become amenable to detailed investigation. The physics of atomic inner shells are peculiar in several respects: (i) The energies are high; for example the 1s binding energy reaches 100 keV at Z=87. Consequently, strong relativistic and quantum electrodynamic effects arise. (ii) Transitions are mostly radiationless, proceed through many channels, and are often very strong; hole state lifetimes thus become as short as attoseconds, with widths measured in tens of electron volts. The dynamics of inner-shell transitions consequently exhibit unusual features. This research program has explored these peculiar properties of energetic inner-shell processes. Attention has been paid to relativistic and quantum-electrodynamic effects and large-scale state-of-the-art computations of hole state energies and transition rates have been made. In the course of this work, there has been developed the first general computer code for the relativistic calculation of Auger rates.</p>											
20. DISTRIBUTION/AVAILABILITY OF ABSTRACT UNCLASSIFIED/UNLIMITED <input checked="" type="checkbox"/> SAME AS RPT. <input checked="" type="checkbox"/> DTIC USERS <input type="checkbox"/>		21. ABSTRACT SECURITY CLASSIFICATION Unclassified									
22a. NAME OF RESPONSIBLE INDIVIDUAL Dr Ralph E. Kelley		22b. TELEPHONE NUMBER <i>(Include Area Code)</i> 202/767-4908	22c. OFFICE SYMBOL NP								

AD-A179 066

DTIC ELECTED

APR 8 1987

A

UNIVERSITY OF OREGON
Department of Physics and Chemical Physics Institute

Final Per REK
~~ANNUAL~~ TECHNICAL REPORT

AIR FORCE OFFICE OF SCIENTIFIC RESEARCH (AFOSR)
NOTICE OF TRANSMITTAL TO DTIC
This technical report has been reviewed and is
approved for public release, so that AFOSR-TR-87-0296-12.
Distribution is unlimited.
MATTHEW J. SANDER
Chief, Technical Information Division

Relativistic Calculations and Measurements
of Energies, Auger Rates, and Lifetimes

Sponsored by
Advanced Research Projects Agency (DOD)
ARPA Order No. 4087

Monitored by
U.S. Air Force Office of Scientific Research
Under Contract #F49620-84-C-0039

Approved for public release;
distribution unlimited.

- (1) ARPA Order 4087
- (2) Program Code 4E20
- (3) Name of Contractor: State of Oregon, acting by and through the State Board of Higher Education on behalf of the University of Oregon
- (4) Effective Date of Contract: 15 January 1984
- (5) Contract Expiration Date: 14 January 1985
- (6) Amount of Contract Dollars: \$200,000
- (7) Contract Number: F49620-84-C-0039
- (8) Principal Investigator: Professor Bernd Crasemann, Phone Number (503) 686-4754
- (9) Program Manager: Dr. Ralph Kelley, AFOSR/NP, Phone Number (202) 767-4904
- (10) Short Title of Work: Relativistic Calculations and Measurements of Energies, Auger Rates, and Lifetimes

The views and conclusions contained in this document are those of the authors and should not be interpreted as necessarily representing the official policies, either expressed or implied, of the Defense Advanced Research Projects Agency or the U.S. Government

15 February 1985

QUALITY INSPECTED
2

Accession For	
NTIS GRA&I	<input checked="" type="checkbox"/>
DTIC TAB	<input type="checkbox"/>
Unannounced	<input type="checkbox"/>
Justification	
By	
Distribution/	
Availability Codes	
Dist	Avail and/or Special
AI	

1. Report Summary

Deep atomic hole states constitute a regime that has only recently become amenable to detailed investigation, thanks to large-scale computers and such energetic probes as synchrotron radiation and accelerated ion beams. The physics of atomic inner shells is peculiar in several respects: (i) The energies are high; e.g., the 1s binding energy reaches 100 keV at $Z=87$. Consequently, strong relativistic and quantum electrodynamic effects arise. (ii) Transitions are mostly radiationless, proceed through many channels, and are often very strong; hole-state lifetimes thus become as short as attoseconds, with widths measured in tens of electron volts. The dynamics of inner-shell transitions consequently exhibit unusual features.

The central purpose of our research program is to explore these peculiar properties of energetic inner-shell processes. We have, in the past, paid particular attention to relativistic and quantum-electrodynamic effects and have performed large-scale state-of-the-art computations of hole-state energies and transition rates. In the course of this work, we have developed the first general computer code for the relativistic calculation of Auger rates.*

At the present time, our primary aim is to gain a better understanding of the dynamics of inner-shell processes, particularly under threshold excitation. It has been known for some years that here the traditional two-step model breaks down, i.e., one cannot treat the decay of a deep inner-shell hole state as separate from its production. The concept breaks down that there is a relaxation phase during which the electrons in the excited atom adjust themselves to the new potential and "forget" how the state was produced. Instead, threshold excitation and decay take place in a single second-order transition, which in essence can be thought of as the inelastic analog of resonance fluorescence. A few years ago, we were able to demonstrate the single-step nature of inner-shell excitation and radiationless deexcitation, dubbed the "resonant Auger Raman effect."² This effect results in resonant emission of sub-natural linewidth radiation.

With the single-step nature of threshold excitation-deexcitation established, and the two-step model long proved valid in the asymptotic limit, the pressing fundamental question is: how does nature link these seemingly contradictory regimes? We have devoted several years to an investigation of this question, and to a search for a unified description that would encompass the entire range of excitation energies.

Related questions with which we have been concerned are (i) the extent and nature of many-body processes associated with atomic inner-shell excitation, (ii) a correct relativistic description of inner-shell ionization by slow charged particles, and of subsequent x-ray emission, and (iii) a search for an explana-

tion why theory almost invariably predicts much too short a lifetime for certain atomic hole states, such as [2s].

We have pursued an integrated theoretical and experimental approach. The theoretical aspect has a strong numerical component. Major computations are being performed at the NASA Ames Research Center, which has a CRAY 1 computer. A professional programmer works half-time for us at NASA ARC. The experimental work is primarily conducted in the Stanford Synchrotron Radiation Laboratory (SSRL), where we operate an on-line gas-phase electron spectrometry system. Data are transferred by magnetic tape to Oregon for analysis on campus.

The major result of the year is the successful outcome of our investigation of the dynamics of inner-shell photoionization and radiationless deexcitation (see Sec. 2.1). Detailed measurements of the Auger resonant Raman effect in the L_3 subshell of xenon and of post-collision interaction (PCI) shifts of the L_3 - M_4M_5 (1G_4) Auger line were completed and successfully explained in the framework of resonant scattering theory. For this purpose, the first fully quantum-mechanical theory of post-collision interaction was constructed. The result is a consistent, unified description of excitation/deexcitation of deep hole states, that incorporates the resonant Raman effect at threshold and asymptotically turns into the two-step model, with PCI providing the link between the two extremes. This result culminates five years of intensive work. Crucial contributors were Teijo Åberg of the Helsinki University of Technology, who spent the fall quarter in our group as a visiting professor and developed the resonant scattering formulation, and Mau Hsiung Chen of the Lawrence Livermore Laboratory, who solved the extremely difficult two-electron continuum wave-function problem.

A related important result of this year's work concerns a many-body effect in inner-shell ionization. A synchrotron-radiation study of double photoionization, through measurements of Auger satellites, permitted us to demonstrate for the first time the theoretically predicted difference between the dependence of shakeup and shakeoff probabilities on the photon energy near threshold (cf. Sec. 2.2).³

We have utilized the large computing power of the NASA ARC facility in order to construct tables of K- and L-shell crosssections for ionization under impact by slow protons, on the basis of a fully relativistic theory that we developed previously⁴ (Sec. 2.3).

Progress was achieved in a protracted theoretical study designed to understand why calculated lifetimes of certain inner-shell hole states (e.g., in the 2s subshell) tend to be very much shorter (by a factor of 2 or 3) than measured. This problem is perplexing because calculations of other lifetimes (or widths) tend to come out well; it is important because the results of such calculations enter into the design of schemes for short-wavelength lasers. Added to previous studies of the effects of

relaxation and intermediate coupling,^{5,6} we have now calculated the effects of final-state channel mixing. The interchannel interaction is found to have a major influence on transition rates (Sec. 2.4).

A calculation of x-ray emission rates for transitions to atomic M-shell vacancies has been completed, with particular emphasis on the results of the choice of gauge.⁷ This is the first systematic relativistic calculation of such rates employing a nonlocal potential (Sec. 2.5).

Our results on dynamical and many-body aspects of inner-shell transitions urgently call for extension of these studies. We plan to carry out further calculations of post-collision interaction to encompass other experimental data obtained recently, and to perform new high-resolution measurements in the threshold region where additional data can provide critical tests of the resonant scattering theory. For this purpose, we hope to gain access to the new 54-pole wiggler line at SSRL, which provides substantially enhanced x-ray flux. Theoretical results on inner-shell transition rates and ionization cross sections also invite significant extensions, building on the recently attained insights.

1. B. Crasemann, M. H. Chen, and H. Mark, *J. Opt. Soc. Am. B* 1, 224 (1984).
2. G. S. Brown, M. H. Chen, B. Crasemann, and G. E. Ice, *Phys. Rev. Lett.* 45, 1937 (1980).
3. G. B. Armen, T. Åberg, K. R. Karim, J. C. Levin, B. Crasemann, G. S. Brown, and G. E. Ice, *Phys. Rev. Lett.* 54, 182 (1985).
4. M. H. Chen, B. Crasemann, and H. Mark, *Phys. Rev. A* 26, 1243 (1982); 27, 2358 (1983).
5. K. R. Karim, M. H. Chen, and B. Crasemann, *Phys. Rev. A* 29, 2605 (1984).
6. K. R. Karim and B. Crasemann, *Phys. Rev. A* 30, 1107 (1984).
7. M. H. Chen and B. Crasemann, *Phys. Rev. A* 30, 170 (1984).

2. Research Results

2.1 Dynamics of atomic inner-shell processes

In threshold excitation of short-lived, deep atomic inner-shell hole states, ionization and decay cannot be treated as distinct processes. Directly at threshold, photoionization and radiationless deexcitation occur in a single process, the resonant Raman effect.¹ Above threshold, excitation and deexcitation are still linked by post-collision interaction (PCI), in which the Auger decay takes place under the influence of the Coulomb field of the receding photoelectron and some of the photoelectron's energy is transferred to the Auger electron. Measurements of the Auger spectrum excited near threshold can therefore probe

the dynamics of inner-shell transitions and provide a stringent test of the semiclassical PCI theory² which has been shown to be valid in the limit of long hole-state lifetimes.³ The first fully quantum-mechanical calculation of PCI becomes possible, based on resonant scattering theory,^{4,5} since the intermediate-state summations can be restricted to states associated with the initial inner-shell hole.

We have performed an investigation in which highly monochromatized, hard synchrotron radiation was tuned through the L_3 threshold of Xe and the $L_3-M_4M_5$ (1G_4) Auger decay including the n ($n \geq 5$) spectator-electron satellite distribution was observed. The peak positions and widths of the $n=5$ and $n=6$ spectator lines were measured as functions of photon energy. The evolution of the M_4M_5 double photoionization peak into the Auger diagram line was found to be strongly blended with the $n \geq 6$ spectator satellites in the excitation-energy range from $E_{exc} = -0.5$ eV to $+5$ eV with reference to the ionization threshold, producing a large apparent PCI shift (-3 eV). We compare this result with predictions from the resonant scattering theory at $E_{exc} = +3$ eV. Above $E_{exc} \approx +5$ eV, the PCI shift is solely due to distortion of the diagram-line shape, so that comparison with both the resonant scattering and semiclassical theories becomes possible.

In the experiment, performed in the Stanford Synchrotron Radiation Laboratory, x rays from an 8-pole wiggler operating at 14 kG were focussed onto a Xe jet by a Pt-coated doubly-curved toroidal mirror. A narrow energy band (-0.6 eV) was selected with a tunable Si (111) (1,-1) double-crystal monochromator. The energy spectrum of electrons emitted from the Xe target was measured with a double-pass cylindrical-mirror analyzer.¹ We take the asymptotic Auger diagram-line energy $\epsilon_A^0 = 3,365.9 \pm 0.2$ eV as reference for the PCI shift. Typical Auger spectra excited at $E_{exc} = -2$ eV and $+1.5$ eV are shown in Fig. 1.

In the resonant scattering theory^{4,5} of the PCI effect, a consistent treatment of threshold phenomena is achieved by interpreting the Auger transition $[n_i l_i] \rightarrow [n_f l_f, n_f' l_f']$ as a resonance in the double electron photoionization of the $n_f l_f$ and $n_f' l_f'$ subshells.⁶ As the incident-photon energy approaches the ionization energy I_i of the $n_i l_i$ threshold, spectator transitions of the type $[n_i l_i] n_l \rightarrow [n_f l_f, n_f' l_f'] n_l$ start to appear owing to $n_i l_i \rightarrow n_l$ excitations. At the threshold, the spectator lines blend into the rapidly increasing double-ionization peak, for which the cross section at large excitation energies $E_{exc} = \omega - I_i$ becomes the product of the $n_i l_i \rightarrow \epsilon l$ single-electron photoionization cross section and the Auger decay probability $\Gamma(\epsilon_A^0)$ for the $[n_i l_i] \rightarrow [n_f l_f, n_f' l_f']^{2S+1}L_J$ transitions with energy ϵ_A^0 . Close to threshold, the Auger decay cannot be treated as an independent process because the emission of the Auger electron is affected by transi-

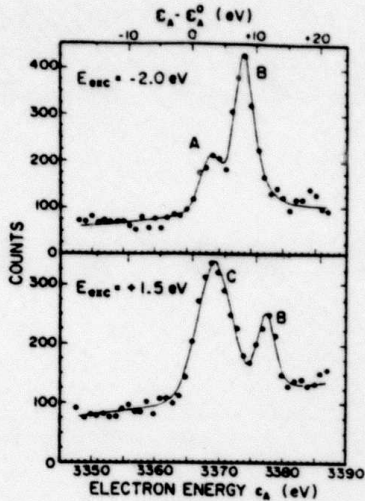


FIG. 1. Xenon $L_3-M_4M_5$ (1G_4) Auger-electron spectrum, excited with synchrotron-radiation photons of energy 2.0 eV below the Xe L_3 binding energy (top) and 1.5 eV above the Xe L_3 binding energy (bottom). Feature A consists primarily of nd ($n \geq 6$) satellites, with a slight admixture of the PCI-shifted diagram line; feature B is the 5d spectator satellite, and feature C consists of the PCI-shifted diagram line, with an admixture of nd ($n \geq 6$) satellites.

tions from the single- to double-hole $n(\ell)l$ states. The double photoionization cross section is

$$\frac{d^2\sigma}{d\epsilon d\epsilon_A} = \frac{4\pi\alpha\omega_0}{3} \Gamma(\epsilon_A^0) \int_0^\infty |\langle \ell | \tau' \rangle|^2 N(\omega - \omega_0) d(\omega - \epsilon - \epsilon_A - I_{ff}), \quad (1)$$

where $N(\omega - \omega_0)$ is the distribution function of the incident photons (normalized to unity), ϵ_A is the Auger-electron energy, and I_{ff} is the ionization energy of the final double-hole state. We have placed the slowly varying factor $\omega_0 \Gamma(\epsilon_A)$ outside the integral. If the continuum wave function $|\ell\rangle$ is replaced by the discrete-state wave function $|n\rangle$ in the overlap matrix element $\langle \ell | \tau' \rangle$, the double-ionization cross section reduces to the cross section $d\sigma_n/d\epsilon_A$ for emitting an Auger electron and placing a spectator electron in the excited state $n1$. In Eq. (1), we have

$$|\tau'\rangle = \sum_{n'=n_{min}}^{\infty} \frac{|n'\rangle \langle n' || r || 0\rangle}{E_{exc} + \epsilon_{n'} + i\Gamma_i/2} + \int_0^\infty \frac{|\tau\rangle \langle \tau || r || 0\rangle d\tau}{E_{exc} - \tau + i\Gamma_i/2}, \quad (2)$$

where each $|\tau(n')\rangle$ must be evaluated in the field of the singly ionized atom with an $n_i l_i$ hole, in contrast to the final $|\ell(n)\rangle$ double-hole states. In Eq. (2), Γ_i is the total decay width of the $[n_i l_i]$ hole state, and $\langle \tau(n') || r || 0\rangle$ is the reduced radial dipole matrix element.

Close to threshold, the Auger-electron emission intensity as a function of ϵ_A is a measure of the cross section

$$\frac{d\sigma}{d\epsilon_A} = \sum_{n=n_{min}}^{\infty} \frac{d\sigma_n}{d\epsilon_A} + \int_0^{\infty} \frac{d^2\sigma}{d\epsilon d\epsilon_A} d\epsilon, \quad (3)$$

which must be convoluted with the spectrometer window function for comparison with the experimental data. If the final double-hole-state lifetime Γ_f^{-1} is taken into account, the Dirac delta function in Eq. (1) is replaced by the normalized density function $(\Gamma_f/2\pi)[(\omega - \epsilon - \epsilon_A - I_{ff'})^2 + \Gamma_f^2/4]^{-1}$. It follows from Eqs. (1) and (2) that for $E_{exc} > 0$ the discrete part of the cross section (3) rapidly vanishes compared with the continuum part $d\sigma_c/d\epsilon_A$.

In the $\Gamma_i > 0$ limit, the corresponding overlap integral $\langle \ell | \tau \rangle$ can be approximated by taking the overlap between two WKB wave functions, corresponding to $\frac{1}{2}k_i^2 = E_{exc} + i(\Gamma_i/2) + V_i(R)$ and $\frac{1}{2}k_f^2 = E_{exc} - \epsilon_A + \epsilon_A^0 + V_f(R)$, respectively.² We have $V_f = 2V_i = R^{-2}$, where the angular-momentum exchange between the photoelectron and the Auger electron is neglected. All semiclassical models of PCI seem to be variants of the WKB approximation, limited to the very-high- n and continuous- ℓ region. Qualitatively, both Eqs. (1)-(3) and the semiclassical approach lead to a transfer of intensity from the low-energy to the high-energy flank of the Auger-electron peak, compared with a Lorentzian shape, resulting in a positive PCI shift. However, whereas in the semiclassical approach the $\epsilon_A - \epsilon_A^0 > E_{exc}$ ($\epsilon < 0$) regime is approached by analytic continuation, the quantum-mechanical theory leads to a spectator-line structure, important in practice for $E_{exc} \lesssim 2\Gamma_i$.

The derivation of Eq. (1) from the general transition matrix formula⁴ is based on a number of approximations. The most severe of these is probably the factorization of the many-electron Hamiltonian matrix element that involves the final two-electron scattering wave function into the one-electron overlap element $\langle \ell | \tau \rangle$ and the Auger-electron probability amplitude.

The cross section (3) was calculated for the $L_3-M_4M_5$ (1G_4) transition with the use of Hartree-Fock (HF) wave functions. Calculation of the continuous part of the function (2) required, for each E_{exc} (3, 10, and 20 eV), 2,000 continuum wave functions $|\tau d\rangle$ in steps of 0.1 eV. These wave functions, as well as the final-state continuum wave functions $|\ell d\rangle$, were generated in the configuration-average frozen HF core, with the exchange interaction taken into account. The summation over the discrete intermediate states was found to be negligible in all three cases.

The ~2.3-eV width of the spectrometer window allows us to resolve only the 5d spectator line in the range $-8\text{eV} < E_{exc} < +5\text{eV}$, at $\Delta(5d) = E_{exc} + 10.5$ eV, from the rest of the structure which appears as a single peak at $\Delta < \Delta(5d)$. Up to $E_{exc} = 0$ eV, Δ appears to follow a linear dispersion law, $\Delta = E_{exc} + 4.0$ eV, which indicates that it is mostly 6d. The linear dependence of $\Delta(5d)$ and $\Delta(6d)$ on E_{exc} is plotted in Fig. 2; the resonance energies are indicated at which the spectator lines gain maximum intensity. According to Eqs. (1)-(3), these resonances occur at $E_{exc} =$

$-\epsilon_n$ or $\Delta(nd) = \epsilon_n - \epsilon_n$. The measured energies ϵ_n agree well with relaxed HF calculations for $n=5$ and 6.

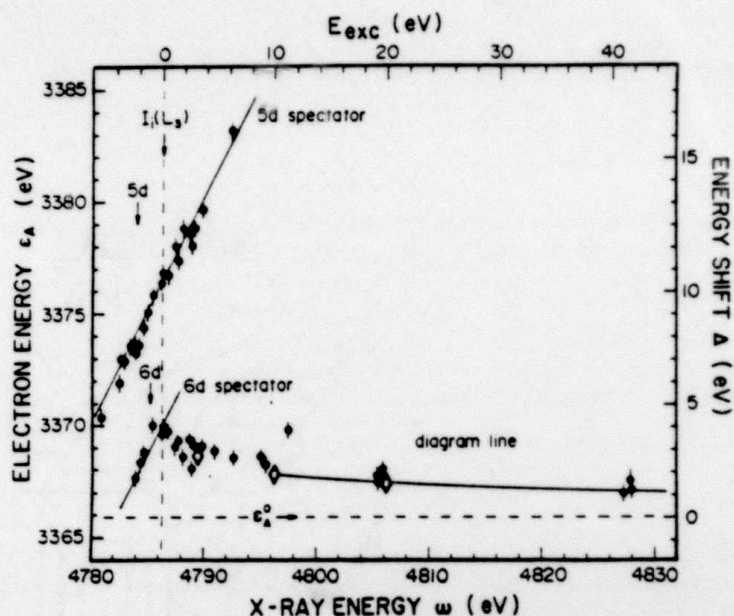


FIG. 2. Xenon $L_3-M_4M_5$ (1G_4) Auger-electron-peak energies, as functions of excitation energy. Experimental data are indicated by solid circles. Diamonds represent the quantum-mechanical shift Δ of the diagram line, while the solid curve indicates the semiclassical shift.

The measured width of the 5d and 6d spectator lines is 4.0 ± 0.5 eV, independently of E_{exc} . This is clearly narrower than the natural width of the $L_3-M_4M_5$ (1G_4) line ($\Gamma_i + \Gamma_f \approx 4.2$ eV),⁷ convoluted with the 2.3-eV wide spectrometer window, i.e., 5.3 eV. This resonance narrowing is in accordance with Eqs. (1)-(3) which, in analogy with the x-ray resonant Raman case,⁵ predict $d\sigma_N/d\epsilon_A \propto N(\omega - \omega_0)$, where $N(\omega - \omega_0)$ is 0.6 eV wide in our experiment.

With the sum rule $\int |\langle \epsilon | \tau' \rangle|^2 d\epsilon = \langle \tau' | \tau' \rangle$, where summation over discrete states is included, it is possible to estimate how much of the low-energy structure represented by peak C in Fig. 1 is due to spectator states. The result, in agreement with the gradual, slow disappearance of the 5d spectator line, is that for $E_{exc} \approx 2\Gamma_i$, the contribution from the discrete final states cannot be neglected. Hence $E_{exc} = +3$ eV represents an intermediate case, in which there is an apparent shift due to the spectators. Experimentally we find $\Delta = 3.0 \pm 0.5$ eV, whereas theory predicts $\Delta = 2.8$ eV after convoluting with the final-state density and the spectrometer window function.

In the calculation of $d\sigma_n/d\epsilon_A$, the discrete portion of complete-set HF computations was approximated by quantum defect theory for both n' (intermediate) and n (final) states ≥ 8 . The summation over intermediate continuum states was found to be important, indicating that there is appreciable recapture of the photoelectron into Rydberg states.

For $E_{exc} > 5$ eV, the quantum-mechanical shape of the Auger diagram line agrees closely with that obtained from the semiclassical Niehaus theory² through numerical integration. After convoluting the theoretical shapes, we find the shifts $\Delta_{theory} = 2.0$ eV, $\Delta_{expt} = 2.5 \pm 0.5$ eV for $E_{exc} = 10$ eV, and $\Delta_{theory} = 1.6$ eV, $\Delta_{expt} = 1.9 \pm 0.7$ eV for $E_{exc} = 20$ eV. It remains to be shown analytically why the Niehaus theory,² if the stationary-phase approximation is not invoked,⁸ leads to almost identically the same results as the quantum-mechanical approach. In Fig. 2, the solid curve for the diagram-line energy represents the function $\Delta = \Delta(E_{exc})$, obtained from the Niehaus theory and convoluted.

Similar measurements as here described have been performed on other wide inner-shell hole states.⁹ Computations are in progress to apply the resonant scattering theory^{4,5} to these cases as well. A preliminary report on this work has been submitted for publication (cf. Sec. 3, Item 12 of this Report).

1. G. S. Brown, M. H. Chen, B. Crasemann, and G. E. Ice, *Phys. Rev. Lett.* **45**, 1937 (1980).
2. A. Niehaus and C. J. Zwakhals, *J. Phys. B* **16**, L135 (1983), and references therein.
3. M. Ya. Amusia, M. Yu. Kuchiev, and S. A. Sheinerman, in Coherence and Correlation in Atomic Collisions, edited by H. Kleinpoppen and J. F. Williams (Plenum, New York, 1980), p. 297.
4. T. Åberg, in Inner-Shell and X-Ray Physics of Atoms and Solids, edited by D. J. Fabian, H. Kleinpoppen, and L. M. Watson (Plenum, New York, 1981), p. 251.
5. T. Åberg and J. Tulkki, in Atomic Inner-Shell Physics, edited by B. Crasemann (Plenum, New York, in press), Chapter 10.
6. We follow the convention of denoting hole states by square brackets, and use atomic units throughout.
7. The width $\Gamma_i = 2.82$ eV was taken from M. H. Chen, B. Crasemann, and H. Mark, *Phys. Rev. A* **24**, 177 (1981); $\Gamma_f \cong 1.4$ eV was estimated from the Xe 3d photoelectron linewidth as given by U. Gelius, *J. Elec. Spect. Rel. Phenom.* **5**, 985 (1974).
8. This approximation has recently been discussed by A. Russek and W. Mehlhorn (submitted for publication in *J. Phys. B*).
9. G. E. Ice, G. S. Brown, G. B. Armen, M. H. Chen, B. Crasemann, J. Levin, and D. Mitchell, in X-Ray and Atomic Inner-Shell Physics--1982, edited by B. Crasemann (AIP Conference Proceedings No. 94, American Institute of Physics, New York, 1982), p. 105.

2.2 Threshold double photoionization of argon with synchrotron radiation.

In atomic inner-shell photoionization, multiple excitation processes occur with significant probability. The resulting final states are approximately described by configurations formed by removal of a core electron and excitation of additional electrons to higher bound states (shakeup) or to the continuum (shakeoff).¹⁻³ Such multiple excitation processes result in satellites in the photoelectron spectra^{1,4-6} and in the Auger and x-ray spectra from transitions through which the photoexcited states decay.^{2,7,8} The study of these multiple excitation processes is important because they epitomize the breakdown of the independent-particle model and can provide important clues for the understanding of electron correlation and of excitation dynamics.^{3,5,9,10} The energy dependence of the cross sections for double excitation is particularly informative near threshold; the observation of Auger satellites makes it possible to measure this dependence. We have performed an investigation in which highly monochromatized, hard synchrotron radiation was tuned through the thresholds for various multiple excitation processes during 1s ionization of Ar, and the probabilities of accompanying 3s and 3p excitation were traced by measuring the intensities of pertinent Auger satellites. Results were compared with theory.^{3,10}

In the experiment, x rays from an 8-pole wiggler, operating at 14 kG, were focused onto an Ar jet by a Pt-coated doubly curved toroidal mirror. The x-ray bandwidth from a Ge (111) double-crystal Bragg monochromator was 0.9 eV at $h\nu=3200$ eV; the flux on target was $\sim 10^{12}$ photons/s with 60 mA of 3-GeV electrons in the SPEAR storage ring. Electron spectra were measured with a computerized double cylindrical-mirror analyzer; with a pass energy of 82.5 eV, the electron-spectrometer resolution was 1.6 eV.

We take the 2,660-eV Ar $K-L_2L_3$ 1D_2 Auger-electron line as reference. The K-LL Auger yield¹¹ of Ar is affected only minutely by excitation of one or two M-shell electrons. The intensity of satellites of the 1D Auger line relative to that of the "diagram" line is therefore a measure of the probability of the multiple photoexcitation processes studied in this work.

To interpret the 1D Auger satellite spectrum it was necessary to calculate the radiationless transition energies and rates in the presence of one or two open M subshells. The initial states can be limited to those which in the sudden approximation are expected to be significantly populated.¹ These are the $[1s3l]$ ($l=0,1$) shakeoff states and the $[1s3l]n_l$ ($n=4$ and 5 for $l=1$, $n=4$ for $l=0$) shakeup states, where square brackets indicate hole states. In the limited $3s(2S)ns^{1,3}3s1s^2S$ and $3p^5(2P)np^{1,3}3s1s^2S$ basis, the eigenstates are linear superpositions of 1S and 3S states. The initial shakeup states can be identified as states with dominant 1S component because the monopole selection rules

prevent transitions to the triplet state. According to our Hartree-Fock (HF) calculations, the initial $[1s3p]4p$ state has almost pure 1S character, whereas in the other shakeup cases the mixture is more uniform.

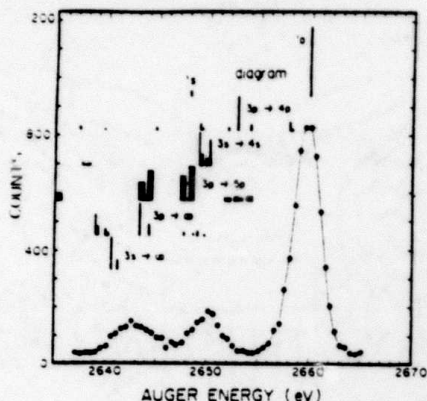


FIG. 3. Calculated energies of Auger satellites caused by 3s- and 3p-electron excitation accompanying 1s ionization, with reference to an Ar K- $L_{2,3}L_{2,3}$ Auger spectrum photoexcited 2,000 eV above the 1s ionization threshold. Estimates of relative satellite intensities within each multiplet are indicated by the heights of the bars.

Calculated Auger satellite energies are indicated schematically in Fig. 3. The satellites arising from 3s and 3p shakeoff accompanying 1s ionization are seen to fall into the peak around ~2,643 eV, while most 3s and 3p shakeup processes cause Auger satellites that fall within the 2,650-eV peak, unresolved from the K- L_2L_2 1S_0 diagram line. The measured intensity of the 1S line, excited below the threshold for any $[1sn]$ double processes, is $11.0 \pm 0.6\%$ of the 1D -line intensity, in excellent agreement with the prediction (11.12%) from a relativistic intermediate-coupling calculation that includes configuration interaction.¹¹ The predicted positions of the Auger lines are only slightly affected by configuration mixing in the initial states and by relativity.

In Fig. 4(a), the relative intensity of the 2,650-eV shakeup satellite peak including the 1S_0 diagram line is plotted. The satellite peak that arises at photon energy $E=3,225$ eV is tentatively ascribed to the $[1s3p]4p^2$ bound-bound resonance, in accordance with the interpretation of the Ar K absorption spectrum⁸ which shows a peak at 3,224 eV. In accord with observations of Kobrin et al.,⁶ the $[1s3p]4p$ shakeup satellite appears to have approximately half its asymptotic intensity at 5 eV above threshold. Saturation of $[1s3p]4p$ plus opening of the $[1s3s]4s$ channel lead to a small gradual increase which levels off to a constant shakeup satellite intensity ~60 eV above the $[1s3p]4p$ threshold.

If we assume in accordance with Fig. 4(a) that the shakeup ratio is practically constant as a function of E , then it can be concluded that the experimental shakeoff curve levels off at high E at $19 \pm 2\%$ (after subtracting the threshold value of 5%). The shape of the curve is well predicted by our calculations using HF

wave functions for both the $[1s3p]$ core and continuum states [Fig. 4(b)]. In the calculation of the continuum wave functions the Lagrangian multipliers were neglected, but a Schmidt orthogo-

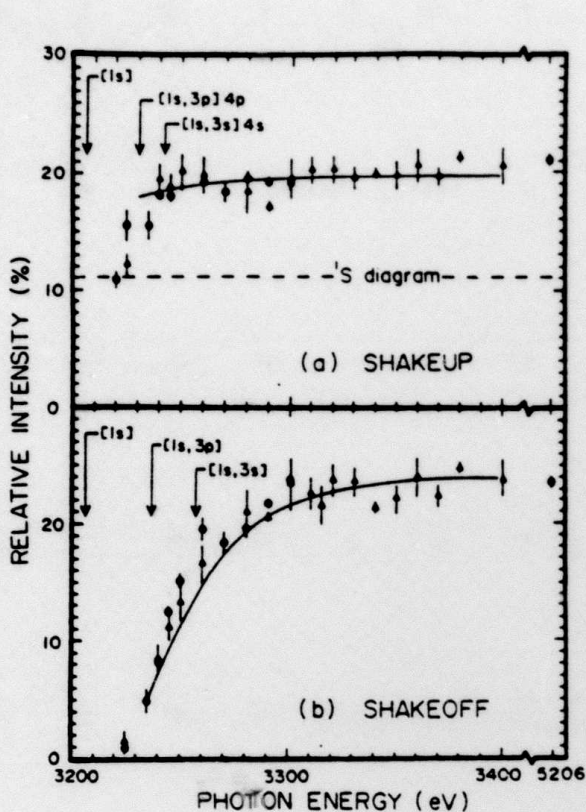


FIG. 4. (a) Intensity of the 2,650-eV feature in the photoexcited Ar $K-L_{2,3}L_{2,3}$ Auger spectrum, with reference to the $1D$ -line intensity, as a function of x-ray energy. The dashed line at 11.1% indicates the $1S$ diagram-line contribution. Energy thresholds for $1s$ ionization and for $3p \rightarrow 4p$ and $3s \rightarrow 4s$ shakeup accompanying $1s$ ionization are indicated by vertical arrows. The normalized theoretical prediction for the near-threshold energy dependence of these relative shakeup probabilities is represented by the solid curve. (b) Photoexcitation-energy dependence of the 2,643-eV Auger satellite-group intensity. Thresholds for $1s$ ionization alone and accompanied by $3p$ and $3s$ ionization are indicated by vertical arrows. The normalized theoretical relative shakeoff probability is indicated by the solid curve. Circles and triangles pertain to data from separate experiments.

nalization was carried out afterwards. As seen in Fig. 4(b), the measured cross-section curve is only slightly affected by the opening of the $[1s3s]$ shakeoff channel. Our calculations predict an asymptotic shakeoff probability of 25% at high E.

We can draw the following conclusions. (1) The difference in the photon-energy dependence of shakeup vs. shakeoff close to threshold has been shown experimentally, for the first time, to be as predicted by theory. (2) The measurements indicate more shakeoff than shakeup at high photon energy, in contrast to the predictions of Ref. 10 but in accord with Ref. 1. (3) The measured shakeup probabilities agree well with the predictions of Ref. 10, but the shakeoff probabilities do not. (4) The measured total shake probabilities are bracketed by the sudden-approximation values calculated by the HF (DF) method for a double-hole $[1s31]$ and a single-hole $[1s]$ field. Within the restricted HF (DF) method, both procedures are somewhat inconsistent with respect to fulfilling the closure relation. This inconsistency could

be removed if many-electron wave functions were used to obtain the

$$\langle \bar{\psi}([1s3l]n(\ell)1)^2 S | \psi_{\text{frozen}}([1s])^2 S \rangle$$

shakeup and shakeoff amplitudes, since the $\bar{\psi}$ functions are eigenfunctions of the same projected (N-1)-electron Hamiltonian $P(N-1)P$, where $P=|1s\rangle\langle 1s|$.

This work was submitted for publication during the period covered by the present Report (cf. Sec. 3, Item 7) and has since been published [Phys. Rev. Lett. 54, 182 (1985)].

1. M. O. Krause, T. A. Carlson, and R. D. Dismukes, Phys. Rev. 170, 37 (1968).
2. T. Åberg, Phys. Rev. 156, 35 (1967).
3. T. Åberg, in Proceedings of the International Conference on Inner-Shell Ionization Phenomena and Future Applications, edited by R. W. Fink, S. T. Manson, J. M. Palms, and P. Venugopala Rao, U.S. AEC Report No. CONF-720404 (Natl. Tech. Information Service, Springfield, Va. 1972), p. 1509.
4. U. Gelius, J. Electron Spectrosc. 5, 985 (1974).
5. R. L. Martin and D. A. Shirley, in Electron Spectroscopy, edited by C. R. Brundle and A. D. Baker (Academic, New York, 1977), Vol. I, Chap. 2.
6. P. H. Kobrin, S. Southworth, C. M. Truesdale, D. W. Lindle, U. Becker, and D. A. Shirley, Phys. Rev. A 29, 194 (1984).
7. L. Asplund, P. Kelfve, B. Blomster, H. Siegbahn, and K. Siegbahn, Phys. Scr. 16, 268 (1977).
8. R. D. Deslattes, R. E. LaVilla, P. L. Cowan, and A. Henins, Phys. Rev. A 27, 923 (1983).
9. M. Ya. Amusia, Adv. At. Mol. Phys. 17, 1 (1981).
10. K. G. Dylla, J. Phys. B 16, 3137 (1983). and 442 (1980).
11. M. H. Chen, B. Crasemann, and H. Mark, Phys. Rev. A 21, 436, 442 (1980).

2.3 Ionization by charged particles

Atomic inner-shell ionization by charged-particle impact has been studied intensively during recent years. The theory has progressed beyond the plane-wave Born approximation, through incorporation of binding and Coulomb-deflection effects.^{1,2} For low-energy collisions, it has been found quite important to include relativity and to employ more realistic wave functions than hydrogenic ones.³⁻¹⁰

Previously tabulated cross sections for atomic inner-shell ionization by charged-particle impact were based on plane-wave Born-approximation (PWBA) calculations with hydrogenic wave functions.¹¹⁻¹² No systematic calculations of inner-shell ionization cross sections have hitherto been published that take into ac-

count the effects of realistic wave functions and that consistently incorporate relativity.

We have drawn upon our previous work on the subject^{4,7,8} and invested a substantial amount of computing time on the NASA Ames Research Center CRAY 1 to prepare tables of relativistic ionization cross sections for K and L shells of 27 elements with atomic numbers $22 < Z < 92$, for proton impact with incident energies from 0.15 to 3 MeV. These cross sections were calculated with Dirac-Hartree-Slater wave functions and include binding, polarization, and Coulomb-deflection corrections.

The work has been accepted for publication in Atomic Data and Nuclear Data Tables (cf. Sec. 3, Item 10).

1. D. H. Madison and E. Merzbacher, in Atomic Inner-Shell Processes, edited by B. Crasemann (Academic, New York, 1975), Vol. I., p. 1.
2. W. Brandt and G. Lapicki, Phys. Rev. A 23, 1717 (1981).
3. G. Lapicki and A. R. Zander, Phys. Rev. A 23, 2072 (1981).
4. M. H. Chen, B. Crasemann, and H. Mark, Phys. Rev. A 26, 1243 (1982).
5. T. Mukoyama and L. Sarkadi, Phys. Rev. A 23, 375 (1981).
6. T. Mukoyama and L. Sarkadi, Phys. Rev. A 25, 1411 (1982).
7. M. H. Chen, B. Crasemann, and H. Mark, Phys. Rev. A 27, 2358 (1983).
8. M. H. Chen, Phys. Rev. A 30, 2082 (1984).
9. O. Benka and A. Kropf, At. Data Nucl. Data Tables 22, 219 (1978).
10. D. Trautman, F. Rösel, and G. Baur, Nucl. Instr. Methods 214, 21 (1983).
11. D. E. Johnson, G. Basbas, and F. D. McDaniel, At. Data Nucl. Data Tables 24, 1 (1979).
12. G. S. Khandelwal, B. H. Choi, and E. Merzbacher, Atomic Data 1, 103 (1969).

2.4 Lifetimes of deep hole states

Atomic inner-shell vacancy states decay predominantly by radiationless processes and, to a minor extent, by radiative transitions. The coupling between radiative and radiationless channels has usually been neglected.¹ The electrostatic coupling between the final K-LL Auger channels in Ne was considered by Howat et al.,^{2,3} and for K-LL, K-LM, and K-MM transitions in Mg by Howat.⁴ These authors found that interchannel coupling substantially alters the spectral distribution of the K Auger electrons which are emitted with kinetic energies of several hundred electron volts. It is tempting, therefore, to investigate similar effects in the case of Coster-Kronig processes which are extremely intense, compared with Auger processes, and in which the outgoing electrons' kinetic energy is at least an order of magnitude less than in Auger transitions.

One inviting case for theoretical investigation is that of L-shell Coster-Kronig transitions in Ar, for which perplexing discrepancies have existed between experimental results^{5,6} and theoretical predictions.⁷⁻¹¹ Hartree,⁷ Hartree-Fock-Slater,⁸ and Hartree-Fock⁹⁻¹⁰ single-configuration calculations have been found to overestimate experimental Ar $L_1-L_{23}M_1$ Coster-Kronig rates by factors of ~4, the $L_1-L_{23}M_1$ to $L_1-L_{23}M_{23}$ intensity ratio by a factor of ~2, and the ratio of $L_1-L_{23}M_1$ (3P_1) to $L_1-L_{23}M_1$ (3P_1) transition rates by a factor of ~120!

Possible reasons for these striking discrepancies in theoretical predictions include (i) many-body interactions in the initial and final atomic systems, (ii) effects of relaxation in the final ionic state, and (iii) effects of the exchange interaction between the continuum electron and the final bound-state electrons. These possibilities have been investigated in recent calculations.⁹⁻¹¹

Mehlhorn¹³ has recently reevaluated his experimental data, leading to a 13% decrease in the $L_1-L_{23}M_1/M_{23}$ intensity ratio. This revised experimental ratio agrees better with theoretical predictions, but the discrepancies remain large in comparison with other atomic transition-rate calculations in which theory tends to come within 10-20% of measured rates.

In an effort to resolve this perplexing situation, we have investigated the effects of continuum interaction in the outgoing channels on the total and relative term intensities of Ar L-shell Coster-Kronig transitions. The rates were calculated through a formulation which includes the effects of final-state channel mixing. The interchannel interaction was found to change individual transition rates by as much as 84%. The relative term intensities from this calculation agree better with experiment than computations which do not take account of channel mixing. The discrepancies previously found between calculated and measured total Coster-Kronig rates and between $^1P/{}^3P$ ratios are largely removed when channel coupling is taken into consideration.

A description of this research has been accepted for publication in Physical Review A (cf. Sec. 3, Item 11); earlier work on this subject has been published in the course of the report year (Sec. 3, Items 2, 4, 6).

1. Interference between radiative and radiationless channels has been considered by L. Armstrong, Jr., C. E. Theodosiou, and M. J. Wall, Phys. Rev. A 18, 2538 (1978); V. L. Jacobs (private communication).
2. G. Howat et al., Phys. Lett. 60A 404 (1977).
3. G. Howat, T. Åberg, and O. Goscinski, J. Phys. B 11, 1575 (1978).
4. G. Howat, J. Phys. B 11, 1589 (1978).
5. W. Mehlhorn, Z. Phys. 208, 1 (1968).

6. J. Nordgren et al., *Physica Scripta* **16**, 70 (1977); **19**, 5 (1979).
7. A. Rubenstein, Ph.D. thesis, University of Illinois, Urbana, 1955 (unpublished).
8. E. J. McGuire, in *Atomic Inner-Shell Processes*, edited by B. Crasemann (Academic, New York, 1975), Vol. I, p. 293; *Phys. Rev. A* **3**, 1801 (1971).
9. K. G. Dyall and F. P. Larkins, *J. Phys. B* **5**, 4103 (1982).
10. K. R. Karim, M. H. Chen, and B. Crasemann, *Phys. Rev. A* **29**, 2605 (1984).
11. J. Bruneau, *J. Phys. B* **16**, 4135 (1983).
12. K. R. Karim and B. Crasemann, *Phys. Rev. A* **30**, 1107 (1984).
13. W. Mehlhorn, private communication.

2.5 X-ray emission from the M shell

Most of the existing calculations of x-ray emission rates deal with transitions to K- and L-shell vacancies. Only one calculation has been performed for M x-ray emission rates, based on relativistic Hartree-Slater wave functions and covering 6 elements with atomic numbers between 48 and 93. We have now performed Dirac-Fock calculations of M x-ray emission rates, both in the Coulomb and length gauges, for 10 elements with atomic numbers between 48 and 92. We have studied the gauge dependence of the M x-ray rates, which is due to the effect of the nonlocal potential. We have explored the effects of relativity on these rates, which are caused by changes in transition energies, shifts in the wave functions, and the role played by higher multipoles. Typical results are illustrated in Fig. 5. This research has been published (Section 3, Item 3.)

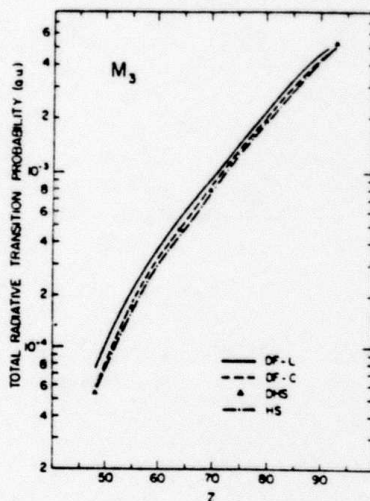


FIG. 5. Total probabilities (in atomic units) of radiative transitions to an M_3 vacancy, as functions of atomic number Z . Results from relativistic Dirac-Fock calculations in the length gauge (DF-L) and in the Coulomb gauge (DF-C) are compared with rates from relativistic local-potential Dirac-Hartree-Slater (DHS) and nonrelativistic Hartree-Slater (HS) calculations.

3. Publications

Published Papers

1. Bernd Crasemann, Mau Hsiung Chen, and Hans Mark: "Atomic Inner-Shell Transitions." J.Opt. Soc. Am B 1, 224 (1984).
2. Kh Rezaul Karim, Mau Hsiung Chen, and Bernd Crasemann: "Effects of Exchange, Electron Correlation, and Relaxation on the $L_1-L_{23}M_1$ Coster-Kronig Spectrum of Argon." Phys. Rev. A 29, 2605 (1984).
3. Mau Hsiung Chen and Bernd Crasemann: "M X-Ray Emission Rates in Dirac-Fock Approximation." Phys. Rev. A 30, 170 (1984).
4. Kh Rezaul Karim and Bernd Crasemann: " $L_1-L_{23}M_1$ Coster-Kronig Spectrum of Argon in Intermediate Coupling." Phys. Rev. A 30, 1107 (1984).
5. Bernd Crasemann and François Wuilleumier: "Atomic Physics with Synchrotron Radiation." PHYSICS TODAY, June 1984, p. 34.
6. Mau Hsiung Chen: "Effects of Relativity and Correlation on L-MM Auger Spectra." Phys. Rev. A 31, 177 (1985).

In Press and Submitted

7. G. Bradley Armen, Teijo Åberg, Kh Rezaul Karim, Jon C. Levin, Bernd Crasemann, George S. Brown, Mau Hsiung Chen, and Gene E. Ice: "Threshold Double Photoionization of Argon with Synchrotron Radiation." Phys. Rev. Lett., in press.
8. Mau Hsiung Chen: "Effects of Relativity and Wave Functions on Atomic L- and M-Shell Ionization by Protons." Phys. Rev. A, in press.
9. Mau Hsiung Chen, Bernd Crasemann, Nils Mårtensson, and Börje Johansson: "Residual Limitations of Theoretical Atomic-Electron Binding Energies." Phys. Rev. A, in press.
10. Mau Hsiung Chen and Bernd Crasemann: "Relativistic Cross Sections for Atomic K- and L-Shell Ionization by Protons, Calculated from a Dirac-Hartree-Slater Model." At. Data Nucl. Data Tables, in press.
11. Kh Rezaul Karim and Bernd Crasemann: "Continuum Interaction in Low-Energy Radiationless Transitions." Phys. Rev. A, in press.

12. G. Bradley Armen, Teijo Åberg, Jon C. Levin, Bernd Crasemann, Mau Hsiung Chen, Gene E. Ice, and George S. Brown: "Threshold Excitation of Short-Lived Atomic Inner-Shell Hole States with Synchrotron Radiation." Submitted to Phys. Rev. Lett.
13. Bernd Crasemann: "Probing Atomic Inner Shells." Text of Plenary Lecture, Proceedings of the X-84 International Conference on X-Ray and Inner-Shell Processes in Atoms, Molecules, and Solids, Leipzig, 1984, edited by A. Meisel. (In press).
14. Bernd Crasemann: "Fluorescence Yields and X-Ray Production from Atomic Inner Shells." Text of Invited Lecture, in Proceedings of the 2nd Workshop on High-Energy Ion-Atom Collision Processes, Debrecen, 1984, edited by D. Berényi (Elsevier, in press).
15. Bernd Crasemann, ed., Atomic Inner-Shell Physics (Plenum, New York, in press).

In Preparation

16. Bernd Crasemann and Gene E. Ice: "Synchrotron Radiation--A Tool for Research." Monograph under contract with Academic Press, New York.

Abstracts

17. Bernd Crasemann: "High-Resolution Spectroscopy in Few-Electron Systems." Abstract of Invited Talk at the Spring Meeting in Washington of the American Physical Society. Bull. Am. Phys. Soc. 29, 730 (1984).
18. Bernd Crasemann and Mau Hsiung Chen: "M X-Ray Emission Rates in Dirac-Fock Approximation." Bull. Am Phys. Soc. 29, 819 (1984).
19. G. Bradley Armen, Mau Hsiung Chen, Bernd Crasemann, Jon C. Levin, George S. Brown, and Gene E. Ice: "Threshold M-Shell Excitation Accompanying K Ionization of Argon." In Satellite Workshop and Conference Abstracts, Ninth International Conference on Atomic Physics, Seattle, Washington, edited by Robert S. Van Dyck, Jr., and E. Norval Fortson. Page B 2.
20. Jon C. Levin, G. Bradley Armen, Mau Hsiung Chen, Bernd Crasemann, Gene E. Ice, and George S. Brown: "Measurements of Post-Collision Interaction in Auger Decay of Deep Hole States." In Satellite Workshop and Conference Abstracts, Ninth International Conference on Atomic Physics, Seattle, Washington, edited by Robert S. Van Dyck, Jr., and E. Norval Fortson. Page B 108.

5. Professional Personnel

Bernd Crasemann, Professor of Physics and Director, Chemical Physics Institute. Principal Investigator.

Teijo Åberg, Visiting Professor of Physics, 15 September to 15 December 1984.

Kh Rezaul Karim, Research Associate.

S. N. Tiwary, Research Associate, 0.5 FTE, 1 January to 30 June 1984.

G. Bradley Armen, Research Assistant

Mahendadasa Yakabadda Gamage, Research Assistant

Jon C. Levin, Research Assistant

Stacey L. Sorensen, Research Assistant (1 July to 31 August 1984 and from 1 January 1985)

Mei Chi Chen, Programmer, 0.5 FTE, from 1 October 1984.

Off-Campus Collaborators:

George S. Brown, Stanford Synchrotron Radiation Laboratory

Mau Hsiung Chen, Lawrence Livermore National Laboratory

Gene E. Ice, Oak Ridge National Laboratory